IEEE Photonics Journal
An IEEE Photonics Society Publication

Open Access

Optical Gain and Laser Characteristics of InGaN Quantum Wells on Ternary InGaN Substrates

Volume 5, Number 2, April 2013

Jing Zhang, Student Member, IEEE
Nelson Tansu, Senior Member, IEEE

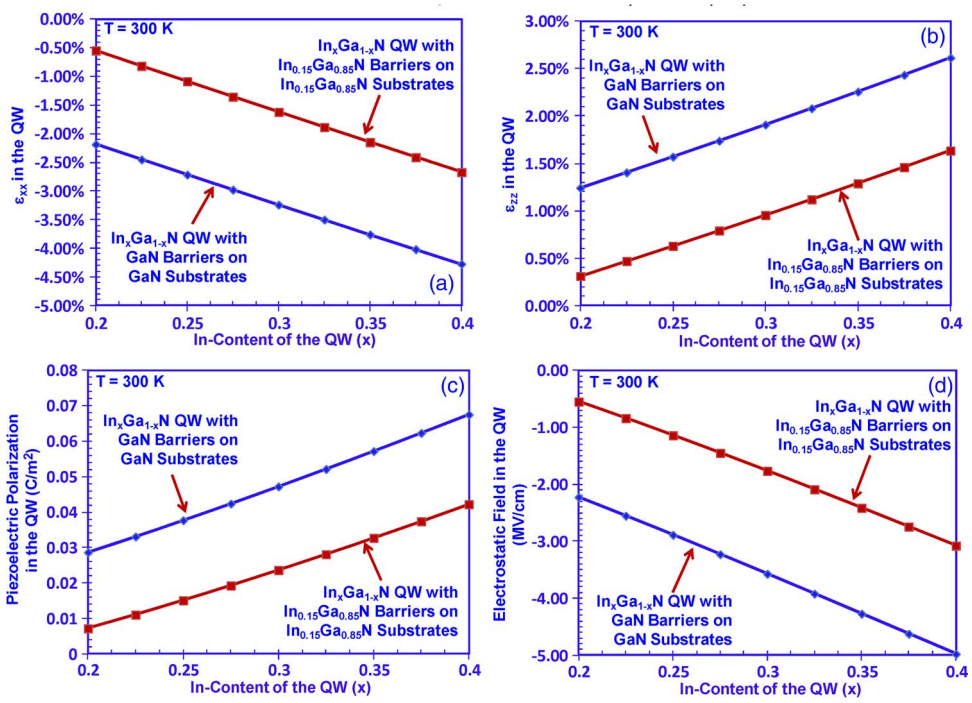

DOI: 10.1109/JPHOT.2013.2247587
1943-0655/$31.00 ©2013 IEEE

IEEE photonics SOCIETY

IEEE

Optical Gain and Laser Characteristics of InGaN Quantum Wells on Ternary InGaN Substrates

Jing Zhang, *Student Member, IEEE*, and Nelson Tansu, *Senior Member, IEEE*

Center for Photonics and Nanoelectronics, Department of Electrical and Computer Engineering, Lehigh University, Bethlehem, PA 18015 USA

DOI: 10.1109/JPHOT.2013.2247587
1943-0655/$31.00 ©2013 IEEE

Manuscript received January 11, 2013; revised February 8, 2013; accepted February 11, 2013. Date of publication February 15, 2013; date of current version March 4, 2013. This work was supported in part by the U.S. National Science Foundation under Grants ECCS 0701421, DMR 0907260, and ECCS 1028490 and in part by the Class of 1961 Professorship Fund. Corresponding author: J. Zhang and N. Tansu (e-mail: jiz209@lehigh.edu; tansu@lehigh.edu).

Abstract: The optical gain and threshold characteristics of InGaN quantum wells (QWs) on ternary InGaN substrate emitting in green and yellow spectral regimes are analyzed. By employing the ternary substrates, the material gains were found as ~3–5 times higher than that of conventional method with reduced wavelength shift. The threshold carrier density is reduced by ~15%–50% from the use of ternary substrate method for green- and yellow-emitting lasers.

Index Terms: III-Nitride, InGaN quantum wells (QWs), ternary InGaN substrate, optical gain, threshold current, laser diodes.

1. Introduction

Significant advances in the III-Nitride materials have led to applications for lasers and light-emitting diodes (LEDs) [1]–[15], thermoelectricity [16], [17], and solar cells [18]. The use of conventional GaN substrate leads to large lattice mismatch strain between the substrate and quantum well (QW). The QW large strain leads to a large internal field in the QW, which reduces the optical matrix element from the charge separation effect [19]–[22]. The large strain also results in increased misfit dislocation density in the high In-content InGaN QWs. To address the charge separation, approaches based on semi/nonpolar InGaN QWs [23]–[27] and InGaN QWs with large overlap design [28]–[36] had been used.

Previous works had reported the growths of InGaN templates and substrates by metalorganic vapor phase epitaxy [37], [38] and hydride vapor phase epitaxy [39]. Recent works [40], [41] had shown the feasibility for accessing the green up to red spectral regimes by using ternary substrate method. Our recent work [42] revealed that the use of ternary InGaN substrates resulted in ~2–3 times increase in the radiative recombination rates for green- and red-emitting InGaN QWs attributing to the reduced charge separation effect. Recent works [43] had also reported an electrically injected semipolar laser grown on an intentionally stress-relaxed n-$In_{0.09}Ga_{0.91}N$ template, which shows the feasibility of the ternary template for lasers. These initial works have shown the potential of this method for achieving high-performance visible LEDs and lasers. However, comprehensive studies on the optical gain and threshold characteristics of InGaN QWs on ternary InGaN substrate or template are still lacking.

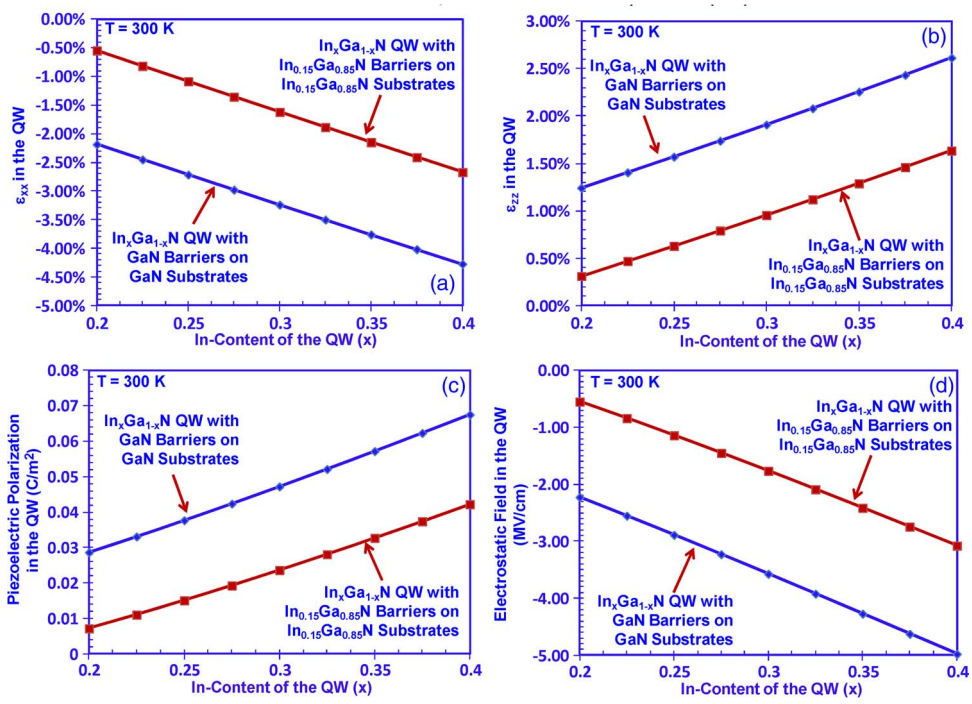

Fig. 1. (a) The strain parameter at *x*-direction, (b) the strain parameter at *z*-direction, (c) the piezoelectric polarization field, and (d) the electrostatic field in the $In_xGa_{1-x}N$ QWs as a function of In-content of the QW, for both $In_xGa_{1-x}N$ QWs with $In_{0.15}Ga_{0.85}N$ barriers on $In_{0.15}Ga_{0.85}N$ substrate and conventional $In_xGa_{1-x}N$ QWs with GaN barriers on GaN substrate.

Here, we present a comprehensive study on the optical gain and threshold characteristics of InGaN QWs on ternary InGaN substrates for green- and yellow-emitting lasers. These results are also compared with those of the conventional InGaN QWs/GaN substrate approach. The band structures and wave functions in this paper were calculated by using self-consistent six-band $\boldsymbol{k} \cdot \boldsymbol{p}$ formalism for wurtzite semiconductor [44]–[47] taking into account the valence band mixing, strain effect, polarization fields, and carrier screening effect, with the band parameters obtained from [47]–[49].

2. Strain and Polarization Field for InGaN QW Lasers With Ternary Substrates

Fig. 1(a) and (b) shows the in-plane (ε_{xx}) and cross-plane (ε_{zz}) strains in the active region layers as a function of In-contents (x) in the $In_xGa_{1-x}N$ QW. The comparisons of the strains in the $In_xGa_{1-x}N$ QWs on $In_{0.15}Ga_{0.85}N$ substrate and conventional GaN substrate for $x = 0.2$ up to $x = 0.4$ were carried out. Attributing to the smaller lattice mismatch, both the ε_{xx} and ε_{zz} are reduced by ~37.5%–75% in the QWs from the use of the ternary substrates, which, in turn, reduces the piezoelectric polarization fields [see Fig. 1(c)] and electrostatic fields [see Fig. 1(d)] in the QWs. The internal fields in the QWs are reduced by ~40% up to 75%, which, in turn, leads to suppression of charge separation [42]. In our studies, all the InGaN QW thicknesses were kept as 3 nm for comparison purposes.

3. Theoretical and Numerical Formulations

The calculations of the band structures and electron and hole wave functions are based on the self-consistent six-band $\boldsymbol{k} \cdot \boldsymbol{p}$ formalism for wurtzite semiconductors [47], which takes into account the valence band mixing, strain effect, spontaneous and piezoelectric polarization, and the carrier screening effect. The spin–orbit interaction is taken into account in the six-band $\boldsymbol{k} \cdot \boldsymbol{p}$ method. The

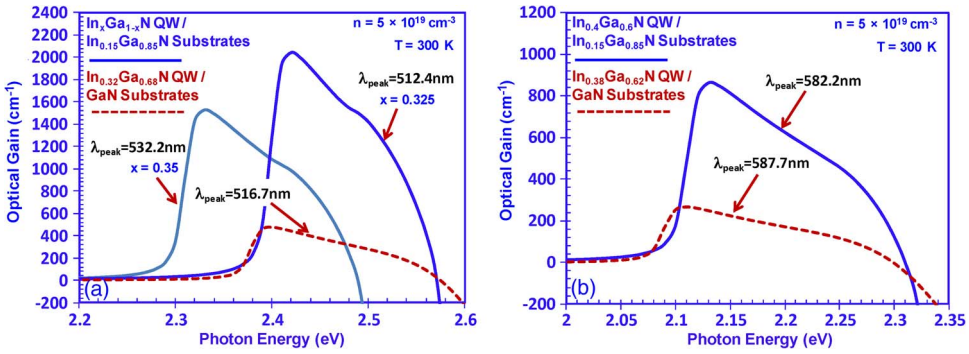

Fig. 2. Optical gain spectra for (a) $In_xGa_{1-x}N$ QWs (x = 0.325, 0.35) with $In_{0.15}Ga_{0.85}N$ barriers on $In_{0.15}Ga_{0.85}N$ substrate, and $In_{0.32}Ga_{0.68}N$ QW with GaN barriers on GaN substrate, and (b) $In_{0.4}Ga_{0.6}N$ QW with $In_{0.15}Ga_{0.85}N$ barriers on $In_{0.15}Ga_{0.85}N$ substrate, and $In_{0.38}Ga_{0.62}N$ QW with GaN barriers on GaN substrate with $n = 5 \times 10^{19}$ cm^{-3} at T = 300 K.

material parameters for GaN, AlN, and InN alloys are taken from [47]–[49] (Table 1 in [47]). The numerical model takes into account the internal electrostatic field resulting from the spontaneous and piezoelectric polarization fields with the details presented in [47]. The calculation of spontaneous and piezoelectric polarization fields follow the treatment discussed in [50] and [51], which do not include the nonlinear term discussed in [52]–[54].

The optical gain calculation is obtained based on the Fermi's Golden rule, including a Lorentzian line-shape function [44], [47]. The upper and lower 3 × 3 Hamiltonian blocks from the 6 × 6 diagonalized Hamiltonian matrix are denoted as $\sigma = \mathrm{U}$ and $\sigma = \mathrm{L}$, respectively. The spontaneous emission rate for transverse-electric (TE) $(e = \mathrm{x})$ or transverse-magnetic (TM) $(e = \mathrm{z})$ polarizations can be obtained by taking into account all interband transitions between nth conduction subbands and mth valence subbands. The optical gain calculation follows the treatment in [44] and [47]

$$g_{sp}^{e}(\hbar\omega) = \frac{2q^2\pi}{n_r c\varepsilon_0 m_0^2 \omega L_w} \sum_{\sigma=U,L} \sum_{n,m} \int \frac{k_t dk_t}{2\pi} \left|(M_e)_{nm}^{\sigma}(k_t)\right|^2 \cdot \frac{f_n^c(k_t)(1 - f_{\sigma m}^v(k_t))(\gamma/\pi)}{\left(E_{\sigma,nm}^{cv}(k_t) - \hbar\omega\right)^2 + \gamma^2} \tag{1}$$

where q is the magnitude of the electron charge, m_0 is the electron mass in free space, and c and ε_0 are the velocity of light and permittivity in free space, respectively. e is the polarization vector of the optical electric field; n_r and L_w are the refractive index and thickness of the QW, respectively. The term $\hbar\gamma$ is the half-linewidth of the Lorentzian function, and the linewidth broadening time $\tau_s = 0.1$ ps $(\gamma = (0.1\ \mathrm{ps})^{-1})$ is used in our calculation [44], [47]. The inhomogeneous broadening is not taken into account here, as there has been no experimental data on this value from the growths of InGaN on ternary substrate. The term $(M_e)_{nm}^{\sigma}(k_t)$ is the momentum matrix element for transitions between the nth conduction-band state and the mth valence-band state.

4. Optical Gain Characteristics of InGaN QWs With Ternary Substrates

The gain properties of the InGaN QWs on ternary and GaN substrates are compared. The In-contents in the InGaN QWs were chosen for similar emission wavelengths at $n \sim 5 \times 10^{19}$ cm^{-3}. Fig. 2(a) shows optical gain spectra for $In_xGa_{1-x}N$ QWs (x = 0.325, 0.35) on $In_{0.15}Ga_{0.85}N$ substrate and conventional $In_{0.32}Ga_{0.68}N$ QW on GaN substrate for green spectral regime. For $In_{0.32}Ga_{0.68}N$ QW on GaN substrate, relatively low material peak gain $(g_{peak} \sim 474.1\ \mathrm{cm}^{-1})$ is obtained with $\lambda_{peak} \sim 516.7$ nm. The material gain is defined as the peak value of the optical gain spectrum. The material gain of the $In_{0.325}Ga_{0.675}N$ QW/$In_{0.15}Ga_{0.85}N$ substrate $(g_{peak} \sim 2039.7\ \mathrm{cm}^{-1})$ is ~3.3 times higher than that of conventional method $(g_{peak} \sim 474.1\ \mathrm{cm}^{-1})$. The material gain of the $In_{0.35}Ga_{0.65}N$ QW/$In_{0.15}Ga_{0.85}N$ substrate $(g_{peak} \sim 1527.7\ \mathrm{cm}^{-1})$ with $\lambda_{peak} \sim 532.2$ nm is ~2.2 times higher than that of the conventional method. For yellow-emitting QWs comparison

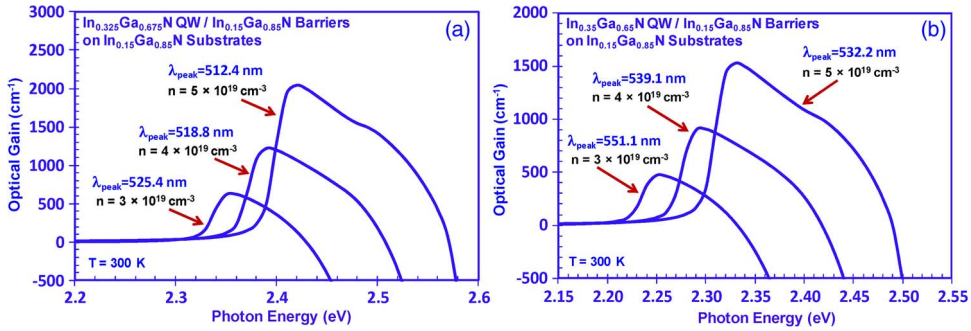

Fig. 3. Optical gain spectra for (a) $In_{0.325}Ga_{0.675}N$ QW, and (b) $In_{0.35}Ga_{0.65}N$ QW with $In_{0.15}Ga_{0.85}N$ barriers on $In_{0.15}Ga_{0.85}N$ substrate for green spectra regime at $n = 3 - 5 \times 10^{19}$ cm^{-3} at room temperature.

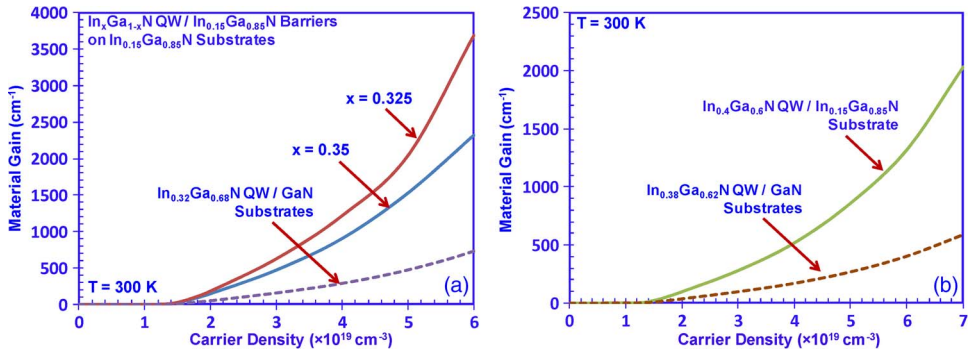

Fig. 4. Comparison of material peak gain as a function of carrier density for (a) $In_xGa_{1-x}N$ QWs ($x = 0.325, 0.35$) on $In_{0.15}Ga_{0.85}N$ substrate, and conventional $In_{0.32}Ga_{0.68}N$ QW on GaN substrate, and (b) $In_{0.4}Ga_{0.6}N$ QW on $In_{0.15}Ga_{0.85}N$ substrate, and conventional $In_{0.38}Ga_{0.62}N$ QW on GaN substrate at room temperature.

[see Fig. 2(b)], the use of the ternary substrate leads to 3.2 times increase in the material gain ($g_{peak} \sim 861.4$ cm^{-1}) over that of the conventional method.

The optical gain spectra for green-emitting InGaN QWs on $In_{0.15}Ga_{0.85}N$ substrate are shown in Fig. 3(a) and (b). The higher In-content QW exhibits lower material gain and larger wavelength blue shift, in comparison with those of lower In-content QW. By comparing the spectra at $n = 3 \times 10^{19}$ cm^{-3} and $n = 5 \times 10^{19}$ cm^{-3}, the wavelength blue shifts for the lower [see Fig. 3(a)] and higher In-content [see Fig. 3(b)] InGaN QW are ~13 nm and ~19 nm, respectively. The corresponding comparisons of the material gains for ternary and conventional methods were shown in Fig. 4(a) and (b) for green- and yellow-emitting QWs, respectively. At higher carrier densities, the material gains for green (yellow)-emitting InGaN QWs on $In_{0.15}Ga_{0.85}N$ substrate are ~3.2–5 times (3.2–3.5 times) higher than that of the conventional method. The improved material gains in green and yellow spectral regimes obtained from the use of ternary substrates are attributed from the reduced charge separation issue in the QWs.

The optical gain properties for InGaN QWs on ternary substrates with various In-contents were shown in Fig. 5(a) and (b). Note that the second peak from the gain spectra of the $In_{0.3}Ga_{0.7}N$ QW/$In_{0.15}Ga_{0.85}N$ substrate at 473.3 nm in Fig. 5(a) is attributed to the band filling effect leading to stronger excited state transitions. The use of higher In-content ternary substrate leads to reduction in charge separation effect in the QW, which results in improved material gain. The material gain for $In_{0.3}Ga_{0.7}N$ QW/$In_{0.15}Ga_{0.85}N$ substrate is ~2135.9 cm^{-1} ($n = 5 \times 10^{19}$ cm^{-3}), which is higher than those employing lower In-content ternary substrates and conventional GaN substrate ($g_{peak} \sim 588.5$ cm^{-1}).

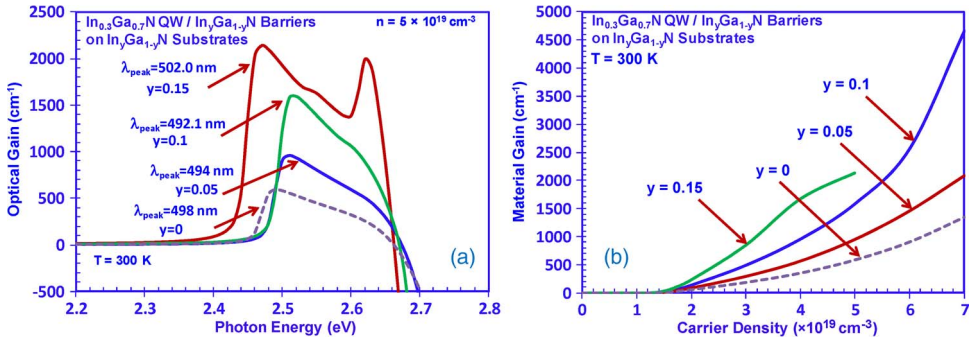

Fig. 5. (a) Optical gain spectra at $n = 5 \times 10^{19}$ cm^{-3} and (b) material gains as a function of carrier density for $In_{0.3}Ga_{0.7}N$ QW with $In_yGa_{1-y}N$ barriers on $In_yGa_{1-y}N$ substrate (y = 0, 0.05, 0.1 and 0.15).

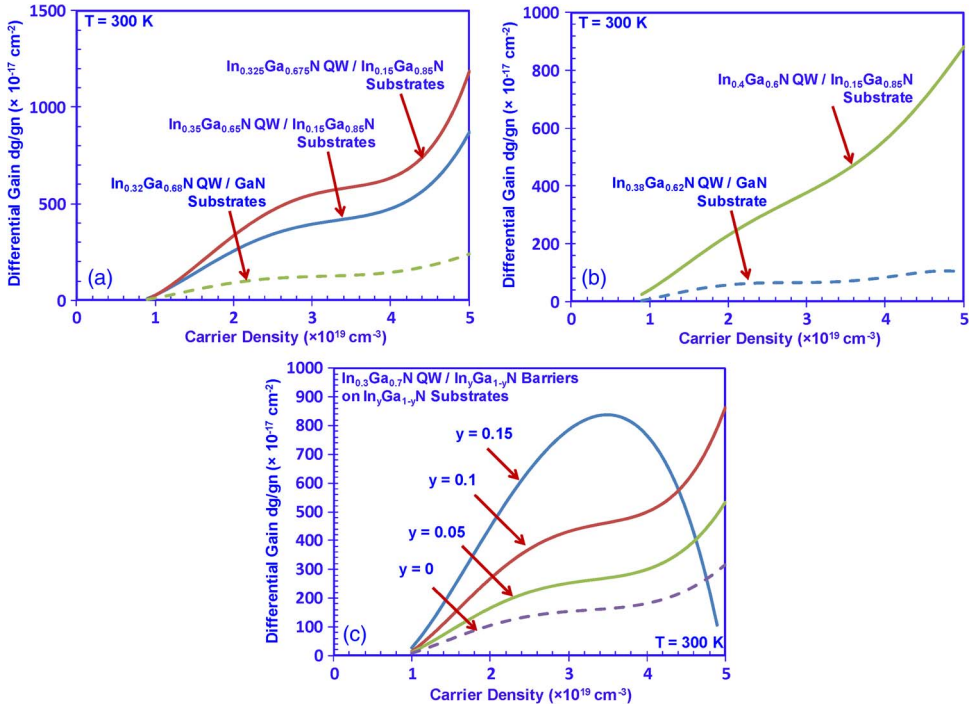

Fig. 6. Differential gain as a function of carrier density for (a) $In_xGa_{1-x}N$ QWs (x = 0.325, 0.35) on $In_{0.15}Ga_{0.85}N$ substrate, and $In_{0.32}Ga_{0.68}N$ QW on GaN substrate, (b) $In_{0.4}Ga_{0.6}N$ QW on $In_{0.15}Ga_{0.85}N$ substrate, and $In_{0.38}Ga_{0.62}N$ QW on GaN substrate, and (c) $In_{0.3}Ga_{0.7}N$ QW with $In_yGa_{1-y}N$ barriers on $In_yGa_{1-y}N$ substrate (y = 0, 0.05, 0.1 and 0.15) at T = 300 K.

5. Differential Gains and Wavelength Shifts Characteristics

The differential gains (dg/dn) for InGaN QWs on ternary and GaN substrates were compared in Fig. 6(a)–(c). Fig. 6(a) shows the dg/dn as a function of carrier density for $In_xGa_{1-x}N$ QWs (x = 0.325, 0.35) on $In_{0.15}Ga_{0.85}N$ substrate and conventional $In_{0.32}Ga_{0.68}N$ QW on GaN substrate for green spectral regime at T = 300 K. The increasing trend of dg/dn for higher carrier density is primarily attributed to the carrier screening effect. The dg/dn for the $In_{0.35}Ga_{0.65}N$ QW and $In_{0.325}Ga_{0.675}N$ QW on $In_{0.15}Ga_{0.85}N$ substrate are ~3.6 and ~4.9 times of that of the conventional $In_{0.32}Ga_{0.68}N$ QW with $n = 5 \times 10^{19}$ cm^{-3}, respectively [see Fig. 6(a)]. For yellow-emitting QWs, the dg/dn for $In_{0.4}Ga_{0.6}N$ QW/$In_{0.15}Ga_{0.85}N$ substrate shows ~7.7 times improvement than that of the $In_{0.38}Ga_{0.62}N$ QW/GaN substrate with $n = 5 \times 10^{19}$ cm^{-3} [see Fig. 6(b)]. The dg/dn are

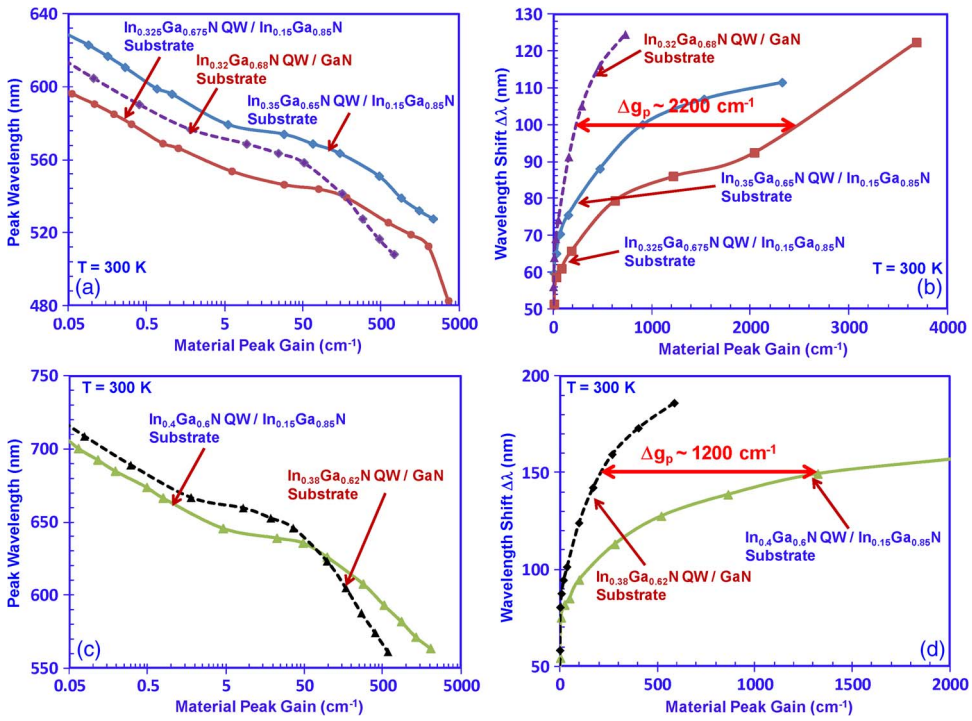

Fig. 7. (a) Peak emission wavelengths from gain spectra as a function of material peak gain, and (b) wavelength shift $\Delta\lambda$ $(\Delta\lambda = \lambda_0 - \lambda(n))$ for $In_xGa_{1-x}N$ QWs $(x = 0.325, 0.35)$ on $In_{0.15}Ga_{0.85}N$ substrate, and conventional $In_{0.32}Ga_{0.68}N$ QW on GaN substrate. (c) Peak emission wavelengths as a function of material peak gain, and (d) wavelength shift $\Delta\lambda$ $(\Delta\lambda = \lambda_0 - \lambda(n))$ for $In_{0.4}Ga_{0.6}N$ QW on $In_{0.15}Ga_{0.85}N$ substrate, and conventional $In_{0.38}Ga_{0.62}N$ QW on GaN substrate at T = 300 K.

compared for $In_{0.3}Ga_{0.7}N$ QW on $In_yGa_{1-y}N$ substrate (y = 0 up to y = 0.15) at T = 300 K [see Fig. 6(c)]. For the use of $In_{0.15}Ga_{0.85}N$ substrate, higher differential gains are achieved for lower carrier densities $(n \sim 3.5 \times 10^{19}\ cm^{-3})$ due to the enhanced matrix element. The decrease in the dg/dn for the ternary substrate with 15% In-content $(n > 3.5 \times 10^{19}\ cm^{-3})$ can be attributed to the band filling effect.

The comparison of the wavelength shifts as a function of material gains for the green- and yellow-emitting QWs on ternary substrates are shown in Fig. 7(a) and (b). For green-emitting QWs [see Fig. 7(a)], the peak emission wavelengths show blue shift for increasing carrier densities for both QWs due to the carrier screening effect. Significantly higher material gains $(g_{peak} > 2000\ cm^{-1})$ are obtained from the use of ternary substrates. In order to compare the wavelength shift quantitatively, the $\Delta\lambda(\Delta\lambda = \lambda_0 - \lambda(n))$ as a function of material peak gains are extracted from Fig. 7(a), where λ_0 is the emission wavelength at $n = 3 \times 10^{18}\ cm^{-3}$ [see Fig. 7(b)]. The use of ternary substrates leads to significantly improved material gain, accompanied with significantly reduced wavelength shift. To illustrate this improvement for $\Delta\lambda \sim 100$ nm, the use of ternary substrate leads to increase in material gain $\sim$2200 cm^{-1} in comparison with that of conventional method. This finding illustrates the feasibility of achieving high material gain with lower carrier density from the use of ternary substrate. Similar finding is also observed for yellow-emitting QWs [see Fig. 7(c) and (d)], which indicates that the increase of $\sim$1200 cm^{-1} in material gain from the use of ternary substrate method for $\Delta\lambda \sim 150$ nm.

The effect of employing different substrates on the screening effect is presented in Fig. 8(a) and (b). Fig. 8(a) compares the peak emission wavelengths as a function of material gain for the $In_{0.3}Ga_{0.7}N$ QW on various $In_yGa_{1-y}N$ substrates (y = 0, 0.05, 0.1, and 0.15). Note that the use of higher In-content substrate leads to larger material gain with reduced wavelength shift [see Fig. 8(b)]. Specifically, for obtaining $g_{peak} \sim 1000\ cm^{-1}$, the lowest wavelength shift $\Delta\lambda \sim 70$ nm is obtained by using $In_{0.15}Ga_{0.85}N$ substrate. In addition, an increase of $\sim$1700 cm^{-1} in material gain is

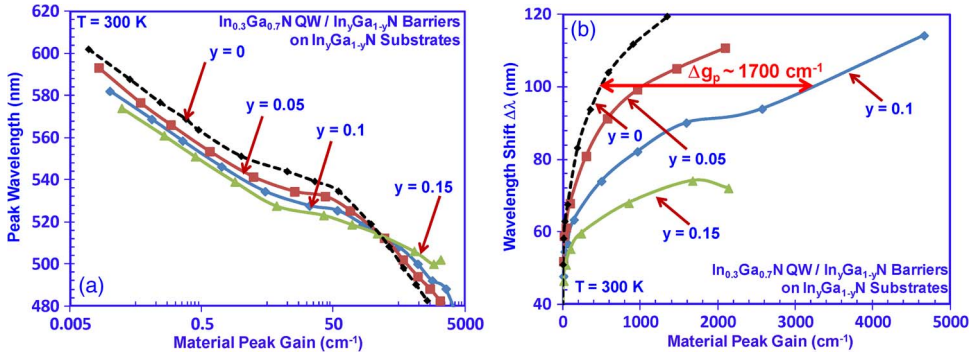

Fig. 8. (a) Peak emission wavelength from gain spectra as a function of material peak gain, and (b) wavelength shift $\Delta\lambda(\Delta\lambda = \lambda_0 - \lambda(n))$ for $In_{0.3}Ga_{0.7}N$ QW with $In_yGa_{1-y}N$ barriers on $In_yGa_{1-y}N$ substrate (y = 0, 0.05, 0.1 and 0.15) at T = 300 K.

obtained by employing the $In_{0.1}Ga_{0.9}N$ substrate as compared with conventional method with $\Delta\lambda \sim 100$ nm.

6. Threshold Characteristics of Green- and Yellow-Emitting Lasers

The threshold characteristics are analyzed for the green- and yellow-emitting lasers using ternary substrates. The threshold gain (g_{th}) is estimated as $\sim$1500 cm^{-1} [47], [55]. The threshold carrier densities (n_{th}) can be obtained from the material peak gain and carrier density relation in Fig. 4(a) and (b). For green-emitting InGaN QWs on ternary substrates [see Fig. 4(a)], the threshold carrier densities are $n_{th} \sim 4.4 \times 10^{19}$ cm^{-3} for $In_{0.325}Ga_{0.675}N$ QW/$In_{0.15}Ga_{0.85}N$ substrate and $n_{th} \sim 4.95 \times 10^{19}$ cm^{-3} for $In_{0.35}Ga_{0.65}N$ QW/$In_{0.15}Ga_{0.85}N$ substrate. In contrast, the material gains obtained from the conventional active regions emitting in green spectral regime at similar carrier density $(n \sim 4.4-6.27 \times 10^{19}$ cm$^{-3})$ range from $\sim$200$-$400 cm^{-1}, which are significantly lower than those obtained from the ternary substrate approach. For yellow-emitting InGaN QWs on ternary substrates [see Fig. 4(b)], the threshold carrier density is $n_{th} \sim 6.27 \times 10^{19}$ cm^{-3}. Similarly, the material gain obtained from the conventional QW at similar carrier density is as low as $\sim$400 cm^{-1}, which indicates that significantly higher carrier density is required for the conventional approach in order to achieve $g_{th} \sim 1500$ cm^{-1}.

The threshold carrier densities of the green-emitting QWs on ternary substrates with various In-contents can be extracted from Fig. 5(b). For $In_{0.3}Ga_{0.7}N$ QW, the n_{th} are $\sim 6.05 \times 10^{19}$ cm^{-3}, 4.9×10^{19} cm^{-3}, and 3.75×10^{19} cm^{-3}, respectively, for $In_{0.05}Ga_{0.95}N$, $In_{0.1}Ga_{0.9}N$, and $In_{0.15}Ga_{0.85}N$ substrates. The corresponding n_{th} for the conventional method is larger than 7×10^{19} cm^{-3}. Note that the increased electron-hole wavefunction overlap in the QWs grown on ternary substrate leads to the enhancement of the radiative recombination rates and optical gains. The low threshold carrier density operation is important for suppressing monomolecular $(\sim A \cdot n_{th})$ and Auger $(\sim C \cdot n_{th}^3)$ recombination current densities at threshold condition. The increased material gain result in reduction in n_{th}, which result in suppression of nonradiative threshold current density $(J_{non\_rad} \sim A \cdot n_{th} + C \cdot n_{th}^3)$ [47] and reduction in total threshold current density $(J_{th} = J_{Rad} + J_{non\_rad})$ for nitride-based lasers on ternary substrates.

To analyze the threshold current densities (J_{th}) for the green- and yellow-emitting lasers, the relation of the material gain as a function of J_{tot} for $In_xGa_{1-x}N$ QWs (x = 0.325, 0.35, and 0.4) on $In_{0.15}Ga_{0.85}N$ substrate are shown in Fig. 9. The monomolecular recombination rates of $A = 6 \times 10^8$ s^{-1}, 1×10^9 s^{-1} and 1.5×10^9 s^{-1} are used similar to [56]. For achieving $g_{th} \sim 1500$ cm^{-1}, yellow-emitting QWs typically have $\sim$30% higher J_{th} over that of green-emitting QWs.

The threshold comparison from the use of ternary $In_yGa_{1-y}N$ substrates (with y = 0.05, 0.1, and 0.15) are presented for various monomolecular recombination rates [see Fig. 10(a)–(c)]. In this comparison, the active region was chosen as $In_{0.3}Ga_{0.7}N$ QW. The reduction in the n_{th} from the ternary substrate is important for suppressing the nonradiative current density, which, in turn,

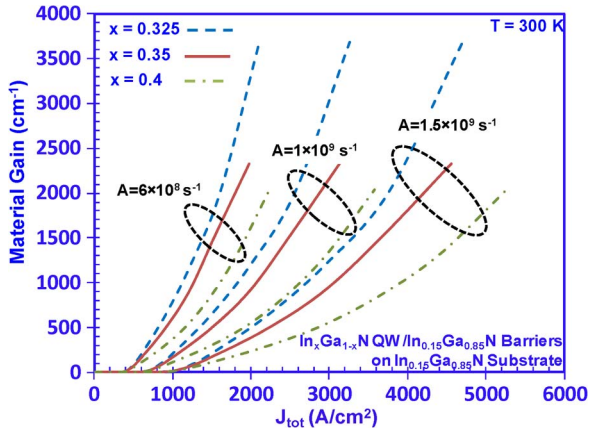

Fig. 9. Material gain as a function of total current density for $In_xGa_{1-x}N$ QWs ($x = 0.325$, 0.35, 0.4) with $In_{0.15}Ga_{0.85}N$ barriers on $In_{0.15}Ga_{0.85}N$ substrate at $T = 300$ K. The monomolecular recombination rates are $A = 6 \times 10^8$ s^{-1}, 1×10^9 s^{-1}, and 1.5×10^9 s^{-1}.

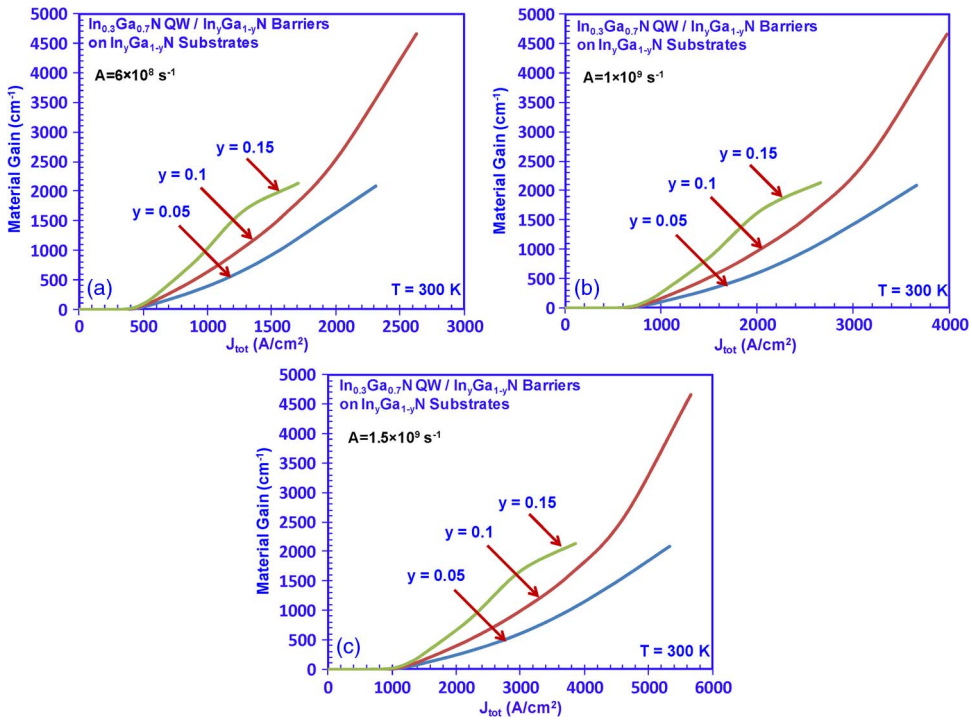

Fig. 10. Material gain as a function of total current density for $In_{0.3}Ga_{0.7}N$ QW with $In_yGa_{1-y}N$ barriers on $In_yGa_{1-y}N$ substrate ($y = 0.05$, 0.1 and 0.15) at $T = 300$ K. The monomolecular recombination rates are (a) $A = 6 \times 10^8$ s^{-1}, (b) $A = 1 \times 10^9$ s^{-1}, and (c) $A = 1.5 \times 10^9$ s^{-1}.

reduces the threshold current density. The threshold analysis here does not take into account the Auger recombination due to the low value of the Auger recombination coefficient ($C_{Auger} \sim 10^{-32}$ cm^6/s) in InGaN [57], [58].

The C_{Auger} values for InGaN semiconductors had been reported with large variation [57]–[62], which range from lower limit ($3.5 \times 10^{-34} - 1 \times 10^{-32}$ cm^6/s) [57], [58] up to higher limit ($1 \times 10^{-31} - 1 \times 10^{-29}$ cm^6/s) [59]–[62]. For the lower limit C_{Auger} of 1×10^{-32} cm^6/s [58], the Auger recombination current densities at threshold ($J_{th\_Auger} \sim n_{th}^3$) range from $\sim$0.025 kA/cm^2 (green QW) up to 0.118 kA/cm^2 (yellow QW), which are negligible (5%) in comparison with the total

threshold current densities for green and yellow lasers using ternary substrates. For the lower limit C_{Auger} of 1×10^{-31} cm^6/sec [61], the J_{th_Auger} range from ~ 0.253 kA/cm^2 (green QW) up to 1.183 kA/cm^2 (yellow QW), which represent 12.3% and 27% of the total threshold current densities for green and yellow lasers using ternary substrates, respectively. Note that the reduction in n_{th} from the use of ternary substrates will be important in reducing the J_{th_Auger} $(\sim n_{th}^3)$ by $\sim$40% up to 85%, in comparison with those of conventional GaN substrate method.

7. Summary

In summary, the optical gain and threshold characteristics of InGaN QWs on ternary InGaN substrates or templates are analyzed for green- and yellow-emitting lasers, which are also compared with the InGaN QWs on conventional GaN substrates or templates. The use of ternary InGaN substrate is expected to result in large increase in material gain and significant reduction in threshold carrier density in the active region, accompanied with less wavelength shift, which may potentially lead to high performance diode lasers emitting in the green and yellow spectral regimes. Note that, experimentally, the successful growths of bulk InGaN substrates have already been realized [37]–[39]. For the InGaN QWs grown on bulk ternary InGaN substrates, the In-contents of the InGaN QWs are lower than that of the substrates. Thus, the growth temperatures of the InGaN QWs should be lower than that of the ternary substrates, which are expected to be kept in good condition during the growths. However, it is important to note that the experimental challenge still needs to be addressed for optimized growths, as the ternary InGaN substrates have only been experimentally realized with In-contents ranging from 0.9% up to 20% [37]–[39].

The development of the ternary substrate still requires further optimization, and the availability of this substrate is the key for enabling the advantages deliberated in this study. In addition, the growths of high In-content InGaN alloy for QW active regions is still challenging, attributed to the increased phase separation issue during the epitaxy.

Acknowledgment

The work was previously presented in IEEE Photonics Conference 2012 (Burlingame, CA, September 2012).

References

[1] M. H. Crawford, "LEDs for solid-state lighting: Performance challenges and recent advances," *IEEE J. Sel. Topics Quantum Electron.*, vol. 15, no. 4, pp. 1028–1040, Jul./Aug. 2009.
[2] Y. K. Ee, J. M. Biser, W. Cao, H. M. Chan, R. P. Vinci, and N. Tansu, "Metalorganic vapor phase epitaxy of III-nitride light-emitting diodes on nanopatterned AGOG sapphire substrate by abbreviated growth mode," *IEEE J. Sel. Topics Quantum Electron.*, vol. 15, no. 4, pp. 1066–1072, Jul./Aug. 2009.
[3] M. Kneissl, D. W. Treat, M. Teepe, N. Miyashita, and N. M. Johnson, "Continuous-wave operation of ultraviolet InGaN/InAlGaN multiple-quantum-well laser diodes," *Appl. Phys. Lett.*, vol. 82, no. 15, pp. 2386–2388, Apr. 2003.
[4] X. Li, S. Kim, E. E. Reuter, S. G. Bishop, and J. J. Coleman, "The incorporation of arsenic in GaN by metalorganic chemical vapor deposition," *Appl. Phys. Lett.*, vol. 72, no. 16, pp. 1990–1992, Apr. 1998.
[5] T. Jung, L. K. Lee, and P.-C. Ku, "Novel epitaxial nanostructures for the improvement of InGaN LEDs efficiency," *IEEE J. Sel. Topics Quantum Electron.*, vol. 15, no. 4, pp. 1073–1079, Jul./Aug. 2009.
[6] X. Li, S. G. Bishop, and J. J. Coleman, "GaN epitaxial lateral overgrowth and optical characterization," *Appl. Phys. Lett.*, vol. 73, no. 9, pp. 1179–1181, Aug. 1998.
[7] W. Guo, A. Banerjee, P. Bhattacharya, and B. S. Ooi, "InGaN/GaN disk-in-nanowire white light emitting diodes on (001) silicon," *Appl. Phys. Lett.*, vol. 98, no. 19, pp. 193102-1–193102-3, May 2011.
[8] X. H. Li, R. B. Song, Y. K. Ee, P. Kumnorkaew, J. F. Gilchrist, and N. Tansu, "Light extraction efficiency and radiation patterns of III-nitride light-emitting diodes with colloidal microlens arrays with various aspect ratios," *IEEE Photon. J.*, vol. 3, no. 3, pp. 489–499, Jun. 2011.
[9] J. Jewell, D. Simeonov, S.-C. Huang, Y.-L. Hu, S. Nakamura, J. Speck, and C. Weisbuch, "Double embedded photonic crystals for extraction of guided light in light-emitting diodes," *Appl. Phys. Lett.*, vol. 100, no. 17, pp. 171105-1–171105-4, Apr. 2012.
[10] J. J. Wierer, A. David, and M. M. Megens, "III-nitride photonic-crystal light-emitting diodes with high extraction efficiency," *Nat. Photon.*, vol. 3, no. 3, pp. 163–169, Mar. 2009.
[11] D. D. Koleske, A. J. Fische, A. A. Allerman, C. C. Mitchell, K. C. Cross, S. R. Kurtz, J. J. Figiel, K. W. Fullmer, and W. G. Breiland, "Improved brightness of 380 nm GaN light emitting diodes through intentional delay of the nucleation island coalescence," *Appl. Phys. Lett.*, vol. 81, no. 11, pp. 1940–1942, Sep. 2002.

[12] M. H. Kim, M. F. Schubert, Q. Dai, J. K. Kim, E. F. Schubert, J. Piprek, and Y. Park, "Origin of efficiency droop in GaN-based light-emitting diodes," *Appl. Phys. Lett.*, vol. 91, no. 18, pp. 183507-1–183507-3, Oct. 2007.
[13] H. Zhao, G. Liu, R. A. Arif, and N. Tansu, "Current injection efficiency induced efficiency-droop in InGaN quantum well light-emitting diodes," *Solid State Electron.*, vol. 54, no. 10, pp. 1119–1124, Oct. 2010.
[14] C. H. Wang, C. C. Ke, C. Y. Lee, S. P. Chang, W. T. Chang, J. C. Li, Z. Y. Li, H. C. Yang, H. C. Kuo, T. C. Lu, and S. C. Wang, "Hole injection and efficiency droop improvement in InGaN/GaN light-emitting diodes by band-engineered electron blocking layer," *Appl. Phys. Lett.*, vol. 97, no. 26, pp. 261103-1–261103-3, Dec. 2010.
[15] J. Piprek, "Efficiency droop in nitride-based light-emitting diodes," *Phys. Stat. Sol. (A), Appl. Mater. Sci.*, vol. 207, no. 10, pp. 2217–2225, Oct. 2010.
[16] J. Zhang, S. Kutlu, G. Y. Liu, and N. Tansu, "High-temperature characteristics of seebeck coefficients for AlInN alloys grown by metalorganic vapor phase epitaxy," *J. Appl. Phys.*, vol. 110, no. 4, pp. 043710-1–043710-6, Aug. 2011.
[17] B. N. Pantha, I-W. Feng, K. Aryal, J. Li, J.-Y. Lin, and H.-X. Jiang, "Erbium-doped AlInGaN alloys as high-temperature thermoelectric materials," *Appl. Phys. Exp.*, vol. 4, no. 5, pp. 051001-1–051001-3, May 2011.
[18] C. J. Neufeld, N. G. Toledo, S. C. Cruz, M. Iza, S. P. DenBaars, and U. K. Mishra, "High quantum efficiency InGaN/GaN solar cells with 2.95 eV band gap," *Appl. Phys. Lett.*, vol. 93, no. 14, pp. 143502-1–143502-3, Oct. 2008.
[19] J. H. Ryou, P. D. Yoder, J. P. Liu, Z. Lochner, H. Kim, S. Choi, H. J. Kim, and R. D. Dupuis, "Control of quantum-confined stark effect in InGaN-based quantum wells," *IEEE J. Sel. Topics Quantum Electron.*, vol. 15, no. 4, pp. 1080–1091, Jul./Aug. 2009.
[20] H. Brown, P. Blood, P. M. Smowton, J. D. Thomson, S. M. Olaizola, A. M. Fox, P. J. Parbrook, and W. W. Chow, "Time evolution of the screening of piezoelectric fields in InGaN quantum wells," *IEEE J. Quantum Electron.*, vol. 42, no. 12, pp. 1202–1208, Dec. 2006.
[21] S. H. Park and S. L. Chuang, "Comparison of zinc-blende and wurtzite GaN semiconductors with spontaneous polarization and piezoelectric field effects," *J. Appl. Phys.*, vol. 87, no. 1, pp. 353–364, Jan. 2000.
[22] A. Venkatachalam, B. Klein, J.-H. Ryou, S. C. Shen, R. D. Dupuis, and P. D. Yoder, "Design strategies for InGaN-based green lasers," *IEEE J. Quantum Electron.*, vol. 46, no. 2, pp. 238–245, Feb. 2010.
[23] S. H. Park, D. Ahn, and S. L. Chuang, "Electronic and optical properties of a- and m-plane Wurtzite InGaN/GaN quantum wells," *IEEE J. Quantum Electron.*, vol. 43, no. 12, pp. 1175–1182, Dec. 2007.
[24] R. M. Farrell, E. C. Young, F. Wu, S. P. DenBaars, and J. S. Speck, "Materials and growth issues for high-performance nonpolar and semipolar light-emitting devices," *Semicond. Sci. Technol.*, vol. 27, no. 2, p. 024001, Feb. 2012.
[25] M. C. Schmidt, K. Kim, R. Farrell, D. F. Feezell, D. Cohen, M. Saito, K. Fujito, J. S. Speck, S. P. Denbaars, and S. Nakamura, "Demonstration of nonpolar m-plane InGaN/GaN laser diodes," *Jpn. J. Appl. Phys.*, vol. 46, no. 8–11, pp. L190–L191, Feb. 2007.
[26] R. M. Farrell, D. F. Feezell, M. C. Schmidt, D. A. Haeger, K. M. Kelchner, K. Iso, H. Yamada, M. Saito, K. Fujito, D. A. Cohen, J. S. Speck, P. DenBaars, and S. Nakamura, "Continuous-wave operation of AlGaN-cladding-free nonpolar m-plane InGaN/GaN laser diodes," *Jpn. J. Appl. Phys.*, vol. 46, no. 29–32, pp. L761–L763, Aug. 2007.
[27] D. Queren, A. Avramescu, G. Bruderl, A. Breidenassel, M. Schillgalies, S. Lutgen, and U. Strau, "500 nm electrically driven InGaN based laser diodes," *Appl. Phys. Lett.*, vol. 94, no. 8, pp. 081119-1–081119-3, Feb. 2009.
[28] R. A. Arif, Y. K. Ee, and N. Tansu, "Polarization engineering via staggered InGaN quantum wells for radiative efficiency enhancement of light emitting diodes," *Appl. Phys. Lett.*, vol. 91, no. 9, pp. 091110-1–091110-3, Aug. 2007.
[29] H. P. Zhao, G. Y. Liu, J. Zhang, J. D. Poplawsky, V. Dierolf, and N. Tansu, "Approaches for high internal quantum efficiency green InGaN light-emitting diodes with large overlap quantum wells," *Opt. Exp.*, vol. 19, no. Suppl. 4, pp. A991–A1007, Jul. 2011.
[30] H. P. Zhao, G. Y. Liu, X. H. Li, R. A. Arif, G. S. Huang, J. D. Poplawsky, S. Tafon Penn, V. Dierolf, and N. Tansu, "Design and characteristics of staggered InGaN quantum well light-emitting diodes in the green spectral regimes," *IET Optoelectron.*, vol. 3, no. 6, pp. 283–295, Dec. 2009.
[31] H. P. Zhao and N. Tansu, "Optical gain characteristics of staggered InGaN quantum well lasers," *J. Appl. Phys.*, vol. 107, no. 11, pp. 113110-1–113110-12, Jun. 2010.
[32] S. H. Park, D. Ahn, B. H. Koo, and J. W. Kim, "Electronic and optical properties of staggered InGaN/InGaN quantum-well light-emitting diodes," *Phys. Stat. Sol. (A)*, vol. 206, no. 11, pp. 2637–2640, Nov. 2009.
[33] S. H. Park, D. Ahn, B. H. Koo, and J. W. Kim, "Dip-shaped InGaN/GaN quantum-well light-emitting diodes with high efficiency," *Appl. Phys. Lett.*, vol. 95, no. 6, pp. 063507-1–063507-3, Aug. 2009.
[34] S. H. Park, D. Ahn, and J. W. Kim, "High-efficiency staggered 530 nm InGaN/InGaN/GaN quantum-well light-emitting diodes," *Appl. Phys. Lett.*, vol. 94, no. 4, pp. 041109-1–041109-3, Jan. 2009.
[35] C. T. Liao, M. C. Tsai, B. T. Liou, S. H. Yen, and Y. K. Kuo, "Improvement in output power of a 460 nm InGaN light-emitting diode using staggered quantum well," *J. Appl. Phys.*, vol. 108, no. 6, pp. 063107-1–063107-6, Sep. 2010.
[36] T. Shioda, H. Yoshida, K. Tachibana, N. Sugiyama, and S. Nunoue, "Enhanced internal quantum efficiency of green LEDs employing AlGaN interlayer in InGaN/GaN MQW structure on sapphire (0001) substrate," in *Proc. 9th Int. Conf. Nitride Semicond.*, Glasgow, U.K., Jul. 2011.
[37] M. Shimizu, T. Kawaguchi, K. Hiramatsu, and N. Sawaki, "MOVPE growth of thick homogeneous InGaN directly on sapphire substrate using AlN buffer layer," *Solid-State Electron.*, vol. 41, no. 2, pp. 145–147, Feb. 1997.
[38] K. Pantzasa, Y. El Gmili, J. Dickerson, S. Gautier, L. Largeau, O. Mauguin, G. Patriarche, S. Suresh, T. Moudakir, C. Bishop, A. Ahaitouf, T. Rivera, C. Tanguy, P. L. Voss, and A. Ougazzaden, "Semibulk InGaN: A novel approach for thick, single phase, epitaxial InGaN layers grown by MOVPE," *J. Cryst. Growth*, Sep. 2012, DOI: 10.1016/j.crysgro.2012.08.041.
[39] [Online]. Available: www.eetimes.com/electronics-news/4189123/TDI-claims-first-InGaN-substrate
[40] T. K. Sharma and E. Towe, "On ternary nitride substrates for visible semiconductor light-emitters," *Appl. Phys. Lett.*, vol. 96, no. 19, pp. 191 105-1–191 105-3, May 2010.
[41] S. H. Park, Y. T. Moon, J. S. Lee, H. K. Kwon, J. S. Park, and D. Ahn, "Spontaneous emission rate of green strain-compensated InGaN/InGaN LEDs using InGaN substrate," *Phys. Stat. Sol. (A)*, vol. 208, no. 1, pp. 195–198, Jan. 2011.

[42] J. Zhang and N. Tansu, "Improvement in spontaneous emission rates for InGaN quantum wells on ternary InGaN substrate for light-emitting diodes," *J. Appl. Phys.*, vol. 110, no. 11, pp. 113110-1–113110-5, Dec. 2011.
[43] P. S. Hsu, M. T. Hardy, F. Wu, I. Koslow, E. C. Young, A. E. Romanov, K. Fujito, D. F. Feezell, S. P. DenBaars, J. S. Speck, and S. Nakamura, "444.9 nm semipolar (1122) laser diode grown on an intentionally stress relaxed InGaN waveguiding layer," *Appl. Phys. Lett.*, vol. 100, no. 2, pp. 021104-1–021104-4, Jan. 2012.
[44] S. L. Chuang, "Optical gain of strained wurtzite GaN quantum-well lasers," *IEEE J. Quantum Electron.*, vol. 32, no. 10, pp. 1791–1800, Oct. 1996.
[45] S. L. Chuang and C. S. Chang, "A band-structure model of strained quantum-well wurtzite semiconductors," *Semicond. Sci. Technol.*, vol. 12, no. 3, pp. 252–263, Mar. 1997.
[46] S. L. Chuang, *Physics of Photonic Devices,* 2nd ed. New York, NY, USA: Wiley, 2009.
[47] H. Zhao, R. A. Arif, Y. K. Ee, and N. Tansu, "Self-consistent analysis of strain-compensated InGaN–AlGaN quantum wells for lasers and light-emitting diodes," *IEEE J. Quantum Electron.*, vol. 45, no. 1, pp. 66–78, Jan. 2009.
[48] I. Vurgaftman and J. R. Meyer, *Nitride Semiconductor Devices*, J. Piprek, Ed. Hoboken, NJ, USA: Wiley, 2007.
[49] I. Vurgaftman and J. R. Meyer, "Band parameters for nitrogen-containing semiconductors," *J. Appl. Phys.*, vol. 94, no. 6, pp. 3675–3696, Sep. 2003.
[50] F. Bernardini and V. Fiorentini, "Spontaneous versus piezoelectric polarization in III–V Nitrides: Conceptual aspects and practical consequences," *Phys. Stat. Sol. (B)*, vol. 216, no. 1, pp. 391–398, Nov. 1999.
[51] O. Ambacher, J. Majewski, C. Miskys, A. Link, M. Hermann, M. Eickhoff, M. Stutzmann, F. Bernardini, V. Fiorentini, V. Tilak, B. Schaff, and L. F. Eastman, "Pyroelectric properties of Al(In)GaN/GaN hetero and quantum well structures," *J. Phys., Condens. Matter*, vol. 14, no. 13, pp. 3399–3434, Apr. 2002.
[52] G. Bester, X. Wu, D. Vanderbilt, and A. Zunger, "Importance of second-order piezoelectric effects in zinc-blende semiconductors," *Phys. Rev. Lett.*, vol. 96, no. 18, pp. 187602-1–187602-4, May 2006.
[53] G. Bester, A. Zunger, X. Wu, and D. Vanderbilt, "Effects of linear and nonlinear piezoelectricity on the electronic properties of InAs/GaAs quantum dots," *Phys. Rev. B*, vol. 74, no. 8, pp. 081305(R)-1–081305(R)-4, Aug. 2006.
[54] J. Pal, G. Tse, V. Haxha, M. A. Migliorato, and S. Tomic, "Importance of non linear piezoelectric effect in Wurtzite III-N semiconductors," *Opt. Quant. Electron.*, vol. 44, no. 3–5, pp. 195–203, Jun. 2012.
[55] H. Y. Ryu, K. H. Ha, S. N. Lee, T. Jang, J. K. Son, H. S. Paek, Y. J. Sung, H. K. Kim, K. S. Kim, O. H. Nam, Y. J. Park, and J. I. Shim, "High-performance blue InGaN laser diodes with single-quantum-well active layers," *IEEE Photon. Technol. Lett.*, vol. 19, no. 21, pp. 1717–1719, Nov. 2007.
[56] W. W. Chow and M. Kneissl, "Laser gain properties of AlGaN quantum wells," *J. Appl. Phys.*, vol. 98, no. 11, pp. 114502-1–114502-6, Dec 2005.
[57] J. Hader, J. V. Moloney, A. Thranhardt, and S. W. Koch, *Nitride Semiconductor Devices*, J. Piprek, Ed. Weinheim, Germany: Wiley-CCH, 2007.
[58] J. Hader, J. V. Moloney, B. Pasenow, S. W. Koch, M. Sabathil, N. Linder, and S. Lutgen, "On the importance of radiative and Auger losses in GaN-based quantum wells," *Appl. Phys. Lett.*, vol. 92, no. 26, pp. 261103-1–261103-3, Jun. 2008.
[59] Y. C. Shen, G. O. Mueller, S. Watanabe, N. F. Gardner, A. Munkholm, and M. R. Krames, "Auger recombination in InGaN measured by photoluminescence," *Appl. Phys. Lett.*, vol. 91, no. 14, pp. 141101-1–141101-3, Oct. 2007.
[60] K. T. Delaney, P. Rinke, and C. G. Van de Walle, "Auger recombination rates in nitrides from first principles," *Appl. Phys. Lett.*, vol. 94, no. 19, pp. 191109-1–191109-3, May 2009.
[61] E. Kioupakis, P. Rinke, K. T. Delaney, and C. G. Van de Walle, "Indirect Auger recombination as a cause of efficiency droop in nitride light emitting diodes," *Appl. Phys. Lett.*, vol. 98, no. 16, pp. 161107-1–161107-3, Apr. 2011.
[62] A. David and M. J. Grundmann, "Droop in InGaN light-emitting diodes: A differential carrier lifetime analysis," *Appl. Phys. Lett.*, vol. 96, no. 10, pp. 103504-1–103504-3, Mar. 2010.